



量子色动力学手征相变及其微观起源

丁亨通

QCD Chiral Phase Transition and Its Microscopic Origin

DING Hengtong

在线阅读 View online: <https://doi.org/10.11804/NuclPhysRev.41.2023CNPC74>

引用格式:

丁亨通. 量子色动力学手征相变及其微观起源[J]. *原子核物理评论*, 2024, 41(1):109–116. doi: 10.11804/NuclPhysRev.41.2023CNPC74

DING Hengtong. QCD Chiral Phase Transition and Its Microscopic Origin[J]. *Nuclear Physics Review*, 2024, 41(1):109–116. doi: 10.11804/NuclPhysRev.41.2023CNPC74

您可能感兴趣的其他文章

Articles you may be interested in

利用格点量子色动力学研究手征平滑过渡温度和手征相变温度

Chiral Crossover and Chiral Phase Transition Temperatures from Lattice QCD

原子核物理评论. 2020, 37(3): 674–678 <https://doi.org/10.11804/NuclPhysRev.37.2019CNPC65>

自旋与手征动力学的运输模拟研究

Studies on Spin and Chiral Dynamics with Transport Simulations

原子核物理评论. 2020, 37(3): 650–659 <https://doi.org/10.11804/NuclPhysRev.37.2019CNPC22>

PNJL模型下手征相变的临界指数

Critical Exponents of the Chiral Phase Transition in the PNJL Model

原子核物理评论. 2020, 37(3): 705–712 <https://doi.org/10.11804/NuclPhysRev.37.2019CNPC23>

A~80核区在束谱学研究进展

Progress on the Spectroscopy in the A~80 Mass Region

原子核物理评论. 2020, 37(1): 11–17 <https://doi.org/10.11804/NuclPhysRev.37.2020001>

强磁场与涡旋场中的夸克胶子物质

Quark Gluon Matter in Strong Magnetic and Vortical Fields

原子核物理评论. 2020, 37(3): 414–425 <https://doi.org/10.11804/NuclPhysRev.37.2019CNPC29>

基于pNJL模型的三维QCD相图

Three-dimensional QCD Phase Diagram in the pNJL Model

原子核物理评论. 2023, 40(4): 493–501 <https://doi.org/10.11804/NuclPhysRev.40.2023025>

QCD Chiral Phase Transition and Its Microscopic Origin

DING Hengtong

(Key Laboratory of Quark and Lepton Physics (MOE) and Institute of Particle Physics,
Central China Normal University, Wuhan 430079, China)

Abstract: The transition of strong-interaction matter from the hadronic phase to the quark-gluon plasma phase is a rapid crossover but not a true phase transition in nature. The true phase transition of strong-interaction matter is expected to exist only in certain limits, *e.g.* chiral limit of massless quarks and *etc.* In this contribution to CNPC2023 Special Issue we present our recent studies on the true phase transition of strong-interaction matter in the chiral limit of massless quarks as well as its microscopic origin. The study is based on (2+1)-flavor lattice QCD simulations using highly improved staggered fermions, with pion masses ranging from 160 MeV down to 55 MeV. Utilizing a newly proposed method to compute the quark mass derivatives of the Dirac eigenvalue spectrum on the lattice, it is found that the axial U(1) anomaly is still manifested at $1.6 T_c$, with a microscopic origin consistent with the dilute instanton gas approximation. Furthermore, based on lattice QCD results and a generalized Banks-Casher relation, it is found that the macroscopic singularity of the chiral phase transition is encoded in the correlation of the Dirac eigenvalue spectrum. Future research directions along these findings are also discussed, including the investigation of the temperature range between T_c and $1.6 T_c$ to understand the breakdown of the dilute instanton gas approximation and its connection to the chiral phase transition.

Key words: QCD phase structure; Dirac eigenvalue spectrum; axial anomaly; chiral symmetry; criticality

CLC number: O571.6 **Document code:** A **DOI:** 10.11804/NuclPhysRev.41.2023CNPC74

0 Introduction

Since the seminal paper titled “Remarks on the chiral phase transition in chromodynamics” by Pisarski and Wilczek in 1984^[1], tremendous progress has been made in our understanding of the phase structure of strong-interaction matter^[2–3]. One of the milestones in studying the phase structure of strong-interaction matter is that it has been established from lattice-regularized Quantum Chromodynamics (QCD) that strong-interaction matter undergoes a rapid crossover transition from the hadronic phase to the quark-gluon plasma phase^[4]. The transition temperature has been determined at a high precision to be $T_{pc} = 156.5(1.5)$ MeV^[5–6], and the temperature at which the chiral phase transition occurs has also been determined recently to be $T_c = 132^{+3}_{-6}$ MeV^[7].

Despite this progress, see *e.g.* Ref. [8], key questions related to the fate of symmetry breaking patterns under extreme conditions of high temperature and large baryon number density as well as other control parameters, and particularly the influence of the axial anomaly on QCD

phase transitions still remain elusive.

In this contribution to CNPC2023 Special Issue we start with our recent findings on the fate of axial U(1) anomaly and its microscopic origin at a temperature high above the chiral phase transition temperature T_c ^[9], and then review our recent results on how the macroscopic criticality is encoded in the microscopic degrees of freedom^[10].

1 The fate of axial U(1) anomaly at high temperature

It has been conjectured that if axial U(1) anomaly is manifested at the chiral phase transition temperature the chiral phase transition will be second order belonging to the O(4) universality class^[1], otherwise the chiral phase transition can even be a first order or a second order belonging to a different universality class^[11–13]. As the relevant physics is highly non-perturbative, the studies using lattice QCD will be important, see recent studies and reviews^[14–21]. However, the fate of the axial U(1) anomaly is still undeter-

Received date: 02 Oct. 2023; **Revised date:** 27 Feb. 2024

Foundation item: National Key Research and Development Program of China (2022YFA1604900); National Natural Science Foundation of China (12293064, 12293060, 12325508)

Biography: DING Hengtong(1983–), male, Qianjiang, Hubei, Professor, working on lattice QCD in extreme conditions of high temperature and large baryon number density as well as other controlled parameters. E-mail: hengtong.ding@cnu.edu.cn

mined. This is mainly due to two main issues in lattice QCD studies. One is that considerable computing resources are required. This is because that one has to take the chiral limit of massless quarks and the continuum limit. The simulation of lattice QCD in the chiral limit becomes significantly costly because the fermion matrix becomes more singular with smaller quark masses and consequently the inversion of the fermion matrix, which is the most time consuming part in lattice QCD computations, involves more numerical work. The other one is the unknown microscopic origin of the axial U(1) anomaly in the proximity of the chiral phase transition temperature. Although the microscopic origin can be inferred from the eigenvalue spectrum $\rho(\lambda)$ of the Dirac fermion matrix there exist difficulties to be elaborated at length. $\rho(\lambda)$ is connected to the order parameter $\langle \bar{\psi}\psi \rangle$ of chiral phase transition, and the signature of axial U(1) anomaly $\chi_\pi - \chi_\delta$ and χ_{disc} as follows

$$\begin{aligned} \langle \bar{\psi}\psi \rangle &= \int_0^\infty \frac{4m\rho(\lambda)}{\lambda^2 + m^2} d\lambda, \\ \chi_\pi - \chi_\delta &= \int_0^\infty \frac{8m^2\rho(\lambda)}{(\lambda^2 + m^2)^2} d\lambda, \\ \chi_{\text{disc}} &= \int_0^\infty \frac{4m\partial\rho/\partial m}{\lambda^2 + m^2} d\lambda. \end{aligned} \quad (1)$$

The Dirac eigenvalue spectrum $\rho(\lambda)$ might have the following forms

$$\rho(\lambda, m) = c_0 + c_1\lambda + c_2m^2\delta(\lambda) + c_3m + c_4m^2 + \mathcal{O}(\lambda, m). \quad (2)$$

Here c_i with $i = 1, 2, 3$ and 4 are parameters which are independent of quark mass (m) and eigenvalue λ . Note that $c_2m^2\delta(\lambda)$ is of most interest as in the chiral limit of massless quarks it makes $\bar{\psi}\psi$ go to zero and $\chi_\pi - \chi_\delta$ and χ_{disc} stay nonzero, *i.e.* it restores the $SU(2) \times SU(2)$ symmetry and breaks the axial U(1) symmetry. However, as quark mass $m \rightarrow 0$ it is hard to observe the contribution from the term *e.g.* $c_2m^2\delta(\lambda)$ since it is m^2 suppressed. Also it is difficult to disentangle the contribution from c_3m and c_4m^2 when m approaches zero.

Concerning the first issue, we performed lattice QCD simulations at a temperature well above the T_c , *i.e.* at $T \simeq 205 \text{ MeV} \simeq 1.6T_c$. At this temperature the simulation is supposed to be cheaper compared to that at temperature in proximity of T_c . If one finds the axial U(1) remains manifested at this $1.6 T_c$, it is natural to deduce that at a lower temperature, *i.e.* T_c , the axial U(1) anomaly also remains manifested with a larger strength. Thus we were able to perform simulations at pion masses much lower compared to the physical one with affordable computing resources. In our lattice QCD simulations we adopted the discretization scheme of highly improved staggered quarks with pion mass ranging from 160 MeV to 55 MeV on

$N_\tau = 8, 12$ and 16 lattices^[9]. This allows us to perform the continuum and chiral extrapolations.

To perform the continuum and chiral extrapolations, we first need to understand the quark mass dependence of $\chi_\pi - \chi_\delta$ and χ_{disc} . In Fig. 1, we show $\chi_\pi - \chi_\delta$ (open points) and χ_{disc} (filled points) as a function of the quark mass ratio m_l/m_s at three different lattice cut-offs. In the high-temperature phase, where chiral symmetry is restored, the QCD partition function should exhibit a $Z(2)$ symmetry and thus be even in quark mass. Consequently, the first-order derivative of the QCD partition function with respect to quark mass, *i.e.*, the chiral condensate, should be odd in quark mass, and the second-order derivative, *i.e.*, χ_{disc} , should be quadratic in quark mass as the chiral limit is approached.

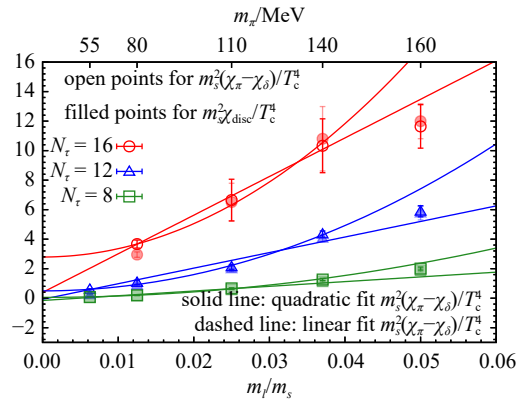


Fig. 1 Quark mass dependence of $\chi_\pi - \chi_\delta$ (open points) and χ_{disc} (filled points) obtained from lattices with $N_\tau = 8, 12$ and 16. (color online)

As seen in Fig. 1, $\chi_\pi - \chi_\delta$ agrees with χ_{disc} within errors, as expected from the restoration of chiral symmetry. Furthermore, we performed fits linear and quadratic in quark mass to $\chi_\pi - \chi_\delta$. These fits are shown as dashed and solid lines in Fig. 1, respectively. The values of $\chi^2/\text{d.o.f.}$ listed in Table 1 indicate that the quadratic behavior in quark mass of $\chi_\pi - \chi_\delta$ is favored. It is worth noting that the difference in $\chi^2/\text{d.o.f.}$ between the linear and quadratic fits is more pronounced in the fits to χ_{disc} and the light quark chiral condensate^[22].

Table 1 Values of $\chi^2/\text{d.o.f.}$ obtained from fits to $\chi_\pi - \chi_\delta$ with $m_\pi < 160 \text{ MeV}$ using ansatzes linear and quadratic in quark mass

$\chi^2/\text{d.o.f.}$	Linear fits in quark mass	Quadratic fits in quark mass
$N_\tau=8$	11.844 3	0.781 243
$N_\tau=12$	7.493 36	0.613 594
$N_\tau=16$	0.058 872 5	0.067 839 2

Based on these findings, we present the continuum and chiral extrapolated results of $\chi_\pi - \chi_\delta$ (top) and χ_{disc} (bottom) in Fig. 2, using a quadratic dependence on quark mass for the chiral extrapolation. It can be seen that in the continuum and chiral limit, $\chi_\pi - \chi_\delta$ and χ_{disc} are nonzero and

consistent with each other. This tells us that the $SU(2) \times SU(2)$ symmetry is restored while the axial $U(1)$ anomaly still remains manifested at $1.6 T_c$. Consequently it is suggested that at T_c the axial $U(1)$ anomaly remains manifested and the chiral phase transition should be of second order belonging to the $O(4)$ universality class.

The observation from Fig. 2 suggests that a term like $c_2 m^2 \delta(\lambda)$ is favored in the Dirac eigenvalue spectrum [Eq. (2)], as it ensures $\chi_\pi - \chi_\delta = \chi_{\text{disc}} \neq 0$. However, as discussed before it is difficult to disentangle the contribution of $c_2 m^2 \delta(\lambda)$ from other terms in $\rho(\lambda)$. One possible way out could be to investigate the n th order derivatives of $\rho(\lambda)$ with respect to quark mass. In the quark mass derivatives of $\rho(\lambda)$ the suppression brought by certain powers of m in the limit of $m \rightarrow 0$ will go away, e.g. $\partial^2(c_2 m^2 \delta(\lambda)) / \partial m^2 = c_2 \delta(\lambda)$.

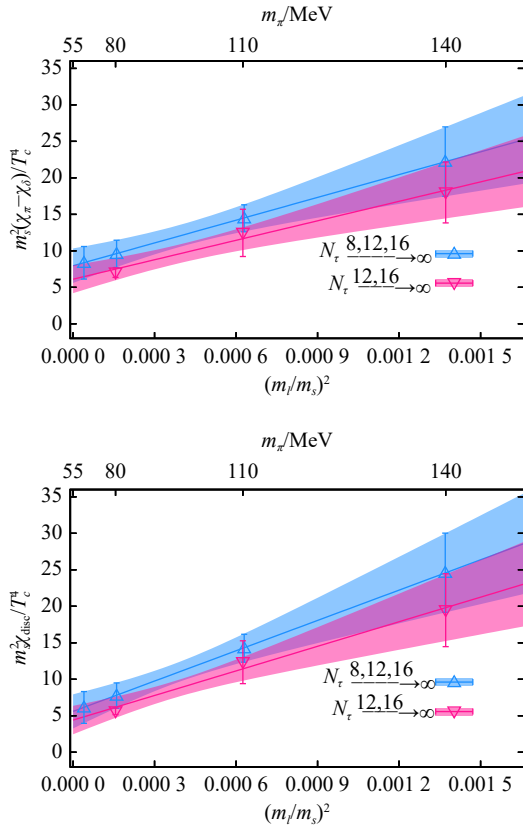


Fig. 2 Continuum and chiral extrapolations for $\chi_\pi - \chi_\delta$ (top) and χ_{disc} (bottom) as function of the quark mass ratio $(m_l/m_s)^2$ at $T \approx 1.6 T_c$. In the chiral limit of massless quarks, i.e. at $(m_l/m_s)^2 = 0$, $\chi_\pi - \chi_\delta$ and χ_{disc} are shown to be nonzero in the continuum limit. The figure is taken from Ref. [9]. (color online)

However, the numerical computation of derivatives is highly non-trivial. For instance,

$$\frac{\partial \rho(\lambda)}{\partial m} = \lim_{\epsilon \rightarrow 0} \frac{\rho(\lambda, m + \epsilon) - \rho(\lambda, m)}{\epsilon} + \mathcal{O}(\epsilon^2), \quad (3)$$

suffers from the discretization error in ϵ . Furthermore, this requires unwanted two sets of lattice QCD simulations at

two different quark masses which should be infinitesimal adjacent.

To avoid the above-mentioned issue in Eq. (3) we proposed a novel method to compute n th order quark mass derivative of $\rho(\lambda)$ without the needs for computing ρ at an additional different quark mass^[9]. Although it seems to be counter-intuitive at first sight the method is straightforward by starting with the definition of $\rho(\lambda)$

$$\rho(\lambda) = \frac{T}{V Z[\mathcal{U}]} \int \mathcal{D}[\mathcal{U}] e^{-S_G[\mathcal{U}]} \det[\mathcal{D}[\mathcal{U}] + m_s] \times (\det[\mathcal{D}[\mathcal{U}] + m_l])^2 \rho_U(\lambda), \quad (4)$$

where $\rho_U(\lambda) = \sum_j \delta(\lambda - \lambda_j)$, and λ_j is the eigenvalue of massless Dirac matrix $\mathcal{D}[\mathcal{U}]$ with a given $SU(3)$ gauge field. Here V is the volume, $S_G[\mathcal{U}]$ is the gauge action and the partition function $Z[\mathcal{U}] = \int \mathcal{D}[\mathcal{U}] e^{-S_G[\mathcal{U}]} \det[\mathcal{D}[\mathcal{U}] + m_s] (\det[\mathcal{D}[\mathcal{U}] + m_l])^2$.

Note that in Eq. (4) only $Z(\mathcal{U})$ and $\det[\mathcal{D}[\mathcal{U}] + m_l]$ depends on the quark mass m_l while ρ_U is independent of m_l . Furthermore, $\det[\mathcal{D}[\mathcal{U}] + m_l]$ can be expressed in terms of Dirac eigenvalues λ as follows

$$\det[\mathcal{D}[\mathcal{U}] + m_l] = \prod_j (+i\lambda_j + m_l)(-i\lambda_j + m_l) = \exp \left\{ \int_0^\infty d\lambda \rho_U(\lambda) \ln [\lambda^2 + m_l^2] \right\}. \quad (5)$$

Thus when taking derivatives of Eq. (4) with respect to m_l with the help of Eq. (5) one can easily obtain the n th order derivative of $\rho(\lambda)$ with respect to m_l . For instance here we list the first and second order derivatives of $\rho(\lambda)$ as follows^[9]

$$\frac{\partial \rho}{\partial m_l} = \frac{T}{V} \int_0^\infty d\lambda_2 \frac{4m_l C_2(\lambda, \lambda_2; m_l)}{\lambda_2^2 + m_l^2}, \quad (6)$$

$$\frac{\partial^2 \rho}{\partial m_l^2} = \frac{T}{V} \int_0^\infty d\lambda_2 \frac{4(\lambda_2^2 - m_l^2) C_2(\lambda, \lambda_2; m_l)}{(\lambda_2^2 + m_l^2)^2} + \frac{T}{V} \int_0^\infty d\lambda_2 d\lambda_3 \frac{(4m_l)^2 C_3(\lambda, \lambda_2, \lambda_3; m_l)}{(\lambda_2^2 + m_l^2)(\lambda_3^2 + m_l^2)}. \quad (7)$$

where C_n is the first order cumulant of n variables $\rho_U(\lambda_1), \rho_U(\lambda_2), \dots, \rho_U(\lambda_n)$. Here C_2 and C_3 can be expressed explicitly as follows^[9, 23]

$$C_2(\lambda, \lambda_2; m_l) = \langle \rho_U(\lambda) \rho_U(\lambda_2) \rangle - \langle \rho_U(\lambda) \rangle \langle \rho_U(\lambda_2) \rangle, \quad (8)$$

$$C_3(\lambda, \lambda_2, \lambda_3; m_l) = \langle \rho_U(\lambda) \rho_U(\lambda_2) \rho_U(\lambda_3) \rangle - \langle \rho_U(\lambda) \rangle \langle \rho_U(\lambda_2) \rho_U(\lambda_3) \rangle - \langle \rho_U(\lambda_2) \rangle \langle \rho_U(\lambda) \rho_U(\lambda_3) \rangle - \langle \rho_U(\lambda_3) \rangle \langle \rho_U(\lambda) \rho_U(\lambda_2) \rangle + 2 \langle \rho_U(\lambda) \rangle \langle \rho_U(\lambda_2) \rangle \langle \rho_U(\lambda_3) \rangle. \quad (9)$$

Note that the derivation of $\partial^n \rho / \partial m_l^n$ is exact without

any assumptions. Once $\rho_U(\lambda)$ is computed using a certain numerical method, *e.g.* Chebyshev filtering method^[24–28], $\partial^n \rho / \partial m_l^n$ can be obtained.

In the top panel of Fig. 3 we show $m_l^{-1} \partial \rho / \partial m_l$ and $\partial^2 \rho / \partial m_l^2$ as a function of λ obtained from lattice QCD simulations with pion mass ranging from 160 MeV to 55 MeV on $N_\tau = 8$ lattices at $T \approx 205$ MeV $\approx 1.6T_c$. It can be clearly seen that $m_l^{-1} \partial \rho / \partial m_l \approx \partial^2 \rho / \partial m_l^2$ and both quantities are almost quark mass independent. A peak structure can also be found in $m_l^{-1} \partial \rho / \partial m_l$ and $\partial^2 \rho / \partial m_l^2$ in the infrared region of λ .

In the insert of the bottom panel of Fig. 3 we show $\partial^3 \rho / \partial m_l^3$ as a function of λ . It can be observed that $\partial^3 \rho / \partial m_l^3 \approx 0$. Together with the observation that $m_l^{-1} \partial \rho / \partial m_l \approx \partial^2 \rho / \partial m_l^2$ it can be deduced that $\rho \propto m_l^2$. As can also be seen that the peak structure in $\partial^2 \rho / \partial m_l^2$ becomes sharper as one approaches the continuum limit with increasing value of N_τ from 8 to 16. This resembles a $\delta(\lambda)$ -like peak structure at the origin. In summary $\rho \propto m_l^2 \delta(\lambda)$ at $1.6T_c$, which is consistent with the manifestation of axial U(1) anomaly in $\chi_\pi - \chi_\delta$ and χ_{disc} and the dilute instanton gas approximation.

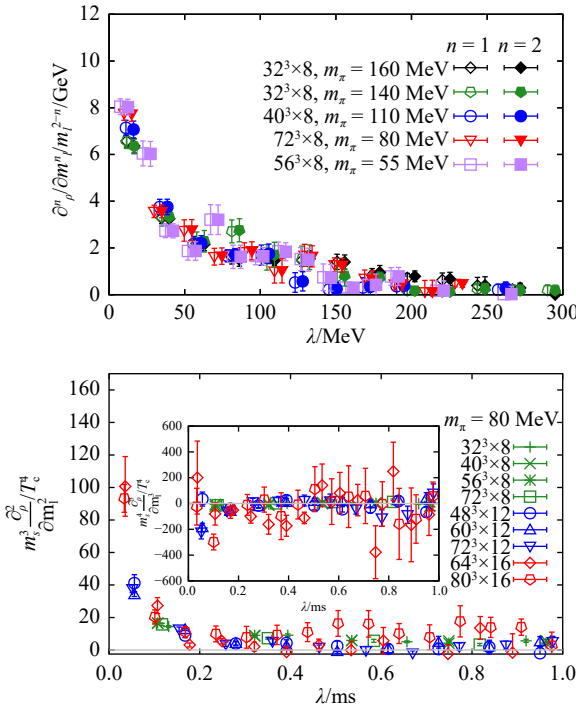


Fig. 3 The derivatives of Dirac eigenvalue spectrum with respect to quark mass. The figure is taken from Ref. [9]. (color online)

2 Microscopic encoding of the macroscopic criticality in the chiral phase transition

As suggested by the studies of the fate of axial U(1) anomaly in the chiral and continuum limit at $1.6T_c$, the

chiral phase transition should be of second order belonging to the O(4) universality class^[9, 22]. In the proximity of a continuous phase transition, the free energy of the system can be decomposed into two parts,

$$F = F_{\text{sing}} + F_{\text{reg}}, \quad (10)$$

where F_{sing} is the singular part of the free energy and overwhelmingly dominates over the regular part F_{reg} . The order parameter M of the phase transition can be defined as the first order derivative of the free energy with respect to an external field H ^[29],

$$M = -\partial F / \partial H = h^{1/\delta} f_1(z), \quad (11)$$

where $h = H/h_0$ and $z = z_0(T - T_c)/T_c H^{-1/\beta\delta}$. Here h_0 and z_0 are non-universal parameters specific for a certain system while β and δ are universal critical exponents. The singular behavior will be more pronounced in higher order derivatives, *e.g.*

$$\chi_{M,n} = -\partial^n F / \partial H^n = \frac{1}{h_0} h^{1/\delta - n+1} f_n(z) \text{ with } n \geq 2. \quad (12)$$

Here f_n is the scaling function, and in the ordinary convention $f_1 \equiv f_G$ and $f_2 \equiv f_\chi$. In the case of QCD, the order parameter of the chiral phase transition is the chiral condensate while the external field is the quark mass. Unlike the case of spin models, in QCD, $\chi_{M,2}$ or $\chi_{M,n}$ also receives the contribution from the connected diagrams, which makes the computation more involved in lattice QCD simulations.

We proposed to investigate the n th order cumulant of chiral condensate^[10],

$$\mathbb{K}_n[\bar{\psi}\psi] = \frac{T}{V} (-1)^n \left. \frac{\partial^n \mathbb{G}(m_l; \epsilon)}{\partial m_l^n} \right|_{\epsilon=m_l}. \quad (13)$$

Here the generating functional $\mathbb{G}(m_l; \epsilon)$ can be defined as

$$\mathbb{G}(m_l; \epsilon) = \ln \langle \exp\{-m_l \bar{\psi}\psi(\epsilon)\} \rangle_0, \quad (14)$$

where $\langle \cdot \rangle_0$ denotes expectation value with respect to the QCD partition function in the chiral limit, $Z(0) = \int \exp(-S[U, 0]) \mathcal{D}[U]$. Since

$$\begin{aligned} \langle \mathcal{O} \rangle &= \frac{1}{Z(m_l)} \int \mathcal{O} \exp(-S[U, m_l]) \mathcal{D}[U] \\ &= \frac{\langle \mathcal{O} \exp\{-m_l \bar{\psi}\psi(m_l)\} \rangle_0}{\langle \exp\{-m_l \bar{\psi}\psi(m_l)\} \rangle_0} \end{aligned} \quad (15)$$

with the QCD partition function $Z(m_l) = \int \exp(-S[U, m_l]) \mathcal{D}[U]$ and $Z(m_l)/Z(0) = \langle \exp\{-m_l \bar{\psi}\psi(m_l)\} \rangle_0$, it is straightforward to find out that \mathbb{K}_n are the standard cumulants of $\bar{\psi}\psi(m_l)$; *e.g.* $\mathbb{K}_1[\bar{\psi}\psi] = T \langle \bar{\psi}\psi(m_l) \rangle / V$, $\mathbb{K}_2[\bar{\psi}\psi] = T \langle [\bar{\psi}\psi(m_l) - \langle \bar{\psi}\psi(m_l) \rangle]^2 \rangle / V$, $\mathbb{K}_3[\bar{\psi}\psi] = T \langle [\bar{\psi}\psi(m_l) - \langle \bar{\psi}\psi(m_l) \rangle]^3 \rangle / V$ *etc.*

The connection of $\mathbb{K}_n[\bar{\psi}\psi]$ to the Dirac eigenvalue λ ,

i.e. energy levels of quarks, is bridged via $\bar{\psi}\psi(\epsilon)$ which is a probe operator for a valence quark with mass ϵ and has a form

$$\bar{\psi}\psi(\epsilon) = 2\text{Tr}[\not{D} + \epsilon]^{-1} \equiv \frac{4\epsilon}{\lambda^2 + \epsilon^2}. \quad (16)$$

By combing Eqs. (13), (14) and (16), one can obtain the expression of \mathbb{K}_n in terms of Dirac eigenvalue spectrum as follows^[10]

$$\mathbb{K}_n[\bar{\psi}\psi] = \int_0^\infty P_n(\lambda) d\lambda, \quad (17)$$

where $P_1(\lambda) = K_1[P_U(\lambda; m_l)]$ for $n = 1$, and for $n \geq 2$

$$P_n(\lambda) = \int_0^\infty K_1[P_U(\lambda; m_l), P_U(\lambda_2; m_l), \dots, P_U(\lambda_n; m_l)] \times \prod_{i=2}^n d\lambda_i. \quad (18)$$

Here K_1 is the first order joint cumulant of n -variables (X_i) defined as

$$K_1(X_1, \dots, X_n) = \frac{T}{V} (-1)^n \left. \frac{\partial^n \ln \langle \prod_{i=1}^n e^{-t_i X_i} \rangle}{\partial t_1 \dots \partial t_n} \right|_{t_1, \dots, t_n=0} \quad (19)$$

and

$$P_U(\lambda; \epsilon) = \frac{4\epsilon\rho_U(\lambda)}{\lambda^2 + \epsilon^2}. \quad (20)$$

Note that in the limit of $\epsilon \rightarrow 0$ $P_U(\lambda; \epsilon)$ is proportional to a delta function. Thus in the chiral limit of massless quarks one can arrive at the following generation of the Banks-Casher formula^[10]

$$\lim_{m \rightarrow 0} \mathbb{K}_n(\bar{\psi}\psi) = (2\pi)^n \mathbb{K}_n[\rho_U(0)]. \quad (21)$$

Based on the above relation, two important questions can be asked. One is what the scaling behavior of \mathbb{K}_n is in the proximity of T_c . The other one is how the scaling behavior of \mathbb{K}_n is encoded in $P_n(\lambda)$ [Eq. (17)]. Concerning the first question, since \mathbb{K}_n is only a part of the n th order susceptibility of the order parameter, a simple conjecture is that \mathbb{K}_n is linearly proportional to the critical behavior encoded in $\chi_{M,n}$ [Eq. (12)], *i.e.*

$$\mathbb{K}_n \propto h^{1/\delta-n+1} f_n(z). \quad (22)$$

Concerning the second question, as seen from the generalized Banks-Casher relation [Eq. (21)], the criticality, if any, must arise from the λ -independent region or the deep infrared part of the eigenvalue spectrum. Based on the first conjecture, one may expect

$$P_n \propto h^{1/\delta-n+1} f_n(z) g(\lambda/m), \quad (23)$$

where all the λ relevant information is encoded in $g(\lambda/m)$.

To check the first conjecture we look in the ratio of cumulant of chiral condensate, *i.e.* $\mathbb{K}_n(z)/\mathbb{K}_n(z=0)$ for

$n=2$ (top) and 3 (Bottom) as a function of z/z_0 . Here $z=0$ means the case at temperature $T=T_c$ since $z=z_0 \frac{T-T_c}{T_c} / H^{1/\beta\delta}$. If the conjecture holds one expects $\mathbb{K}_n(z)/\mathbb{K}_n(z=0) = f_n(z)/f_n(0)$ in terms of z or z/z_0 is independent on the quark mass dependent and temperature. This is exactly what is seen in Fig. 4 in the window of $z/z_0 \in (-0.2, 0.2)$. Note that although z_0 is an undetermined non-universal parameter of QCD in the range of $z/z_0 \in (-0.2, 0.2)$ $f_n(z)/f_n(0)$ is almost independent on the value of z_0 . While outside the window of $z/z_0 \in (-0.2, 0.2)$ we see the data points at various temperature and pion masses do not overlap each other anymore. We can also see in the inserts of Fig. 4 that $\mathbb{K}_n(z)$ rescaled by $H^{1/\delta-n+1}$ is also quark mass and temperature independent in the same region of z/z_0 . Thus the results shown in Fig. 4 suggests $\mathbb{K}_n(z) \propto H^{1/\delta-n+1} f_n(z)$. It is worth mentioning that our approach to investigating these cumulant ratios complements the study of the magnetic equation of state, which is typically conducted using the chiral condensate and its susceptibilities. In the latter case, careful modeling of the regular configurations is important^[30–31]. However, in our approach, we do not need to compute connected susceptibilities; instead, we rely solely on the cumulants of the chiral

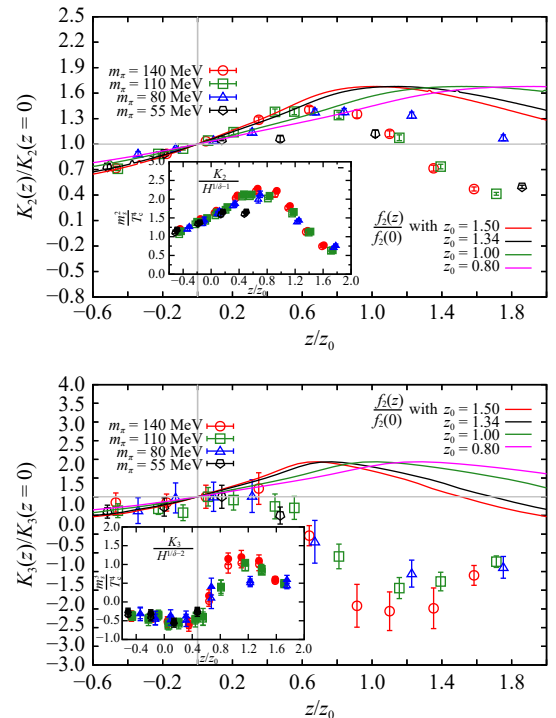


Fig. 4 $\mathbb{K}_n(z)/\mathbb{K}_n(0)$ as a function of $z/z_0 = \frac{T-T_c}{T_c} / H^{1/\beta\delta}$ with $n=2$ (top) and $n=3$ (Bottom) for pion mass ranging from 140 MeV to 55 MeV in the proximity of chiral phase transition temperature. The broken lines show $f_n(z)/f_n(0)$ with various values of undetermined z_0 . The inserts show ratios of $\frac{m_\pi^3}{T_c^3} \frac{T}{V} \mathbb{K}_n(z) / H^{1/\delta-n+1}$ as a function of z/z_0 where the prefactors of $\mathbb{K}_n(z)$ are used to make the quantity renormalization group invariant. (color online)

condensates, where the regular contributions are expected to be mild.

To check the second conjecture, since the relevant infrared energy scale should be $\lambda \sim m_l$ for small values of m_l as expected from the generalized Banks-Casher relation [Eq. (21)] we express all quantities as functions of the dimensionless and renormalization group invariant λ/m_l

$$\begin{aligned} \hat{\lambda} &= \lambda/m_l, \quad \hat{m}_l = m_l/m_s, z = z_0 \hat{m}_l^{-1/\beta\delta} (T - T_c)/T_c, \\ \hat{P}_n(\hat{\lambda}) &= m_s^{n+1} \hat{m}_l P_n(\lambda)/T_c^4, \quad \text{and} \\ \hat{\mathbb{K}}_n[\bar{\psi}\psi] &= \int_0^\infty \hat{P}_n(\hat{\lambda}) d\hat{\lambda} \sim \hat{m}_l^{1/\delta-n+1} f_n(z), \end{aligned} \quad (24)$$

where the dimensionless and renormalization group invariant $\hat{\mathbb{K}}_n[\bar{\psi}\psi] = m_s^n \mathbb{K}_n[\bar{\psi}\psi]/T_c^4$.

In Fig. 5 we show $\hat{P}_n(\hat{\lambda})$ for $n=1$ (left), 2 (middle) and 3 (right) as a function of $\hat{\lambda} \equiv \lambda/m$ in the proximity of $T_c = 144.2(6)$ MeV on $N_\tau = 8$ lattices^[32]. These $\hat{P}_n(\hat{\lambda})$ can reproduce $\hat{\mathbb{K}}_n$ as shown in the inserts of Fig. 4. It can be seen that $\hat{P}_n(\hat{\lambda})$ rapidly goes to zero with increasing $\hat{\lambda}$ at $\hat{\lambda} \sim 1$, and the regions where $\hat{P}_n(\hat{\lambda})$ is nonzero get smaller with increasing n . This reinforces that the relevant infrared energy scale turn out to be $\hat{\lambda} \sim 1$ as indicated from the generalized Banks-Casher relation. In this deep infrared region $\hat{P}_n(\hat{\lambda})$ at a fixed temperature shows clear dependences on m_l . These dependences becomes stronger for increasing n . Meanwhile the form of m_l -dependence of

$\hat{P}_n(\hat{\lambda})$ also changes with varying values of temperature. As also seen from Fig. 5 it is expected that our results become increasingly noisy with increasing n and decreasing m_l .

As discussed before, the m_l and T dependence of $\hat{P}_n(\hat{\lambda})$ shown in Fig. 5 could be understood in terms of the 3-dimensional $O(2)$ scaling property, cf. Eq. (24). To obtain $f_n(z)$ we adopted the system-specific parameters $T_c = 144.2(6)$ MeV and $z_0 = 1.83(9)$ from Ref. [32], where 3-dimensional $O(2)$ scaling fits were carried out for the same lattice ensembles but using an entirely different macroscopic observable, namely the m_l dependence of the static quark free energy. As seen from Fig. 6 once the $\hat{P}_n(\hat{\lambda})$ are rescaled with respective $\hat{m}_l^{1/\delta+1-n} f_n(z)$ the data points in Fig. 5 collapse onto each other, *i.e.* $\hat{P}_n(\hat{\lambda})/(\hat{m}_l^{1/\delta+1-n} f_n(z))$ as a function of $\hat{\lambda}$ is independent of quark mass and temperature for $n = 1, 2$ and 3.

Thus, according to the observation from Fig. 5 and Fig. 6 the macroscopic criticality of chiral phase transition is encoded microscopically in terms of Dirac eigenvalues and their correlations as follows

$$\hat{P}_n(\hat{\lambda}) = \hat{m}_l^{1/\delta-n+1} f_n(z) \hat{g}_n(\hat{\lambda}), \quad (25)$$

where $\hat{g}_n(\hat{\lambda})$ characterize the system-specific of the n th order energy-level correlations. As inferred from our generalized Banks-Casher relations of Eq. (21) the $\hat{g}_n(\hat{\lambda})$ must also satisfy $\lim_{V \rightarrow \infty} \lim_{a \rightarrow 0} \lim_{m_l \rightarrow 0} \hat{g}_n(\hat{\lambda}) \rightarrow \delta(\hat{\lambda})$, such that $\hat{\mathbb{K}}_n[\bar{\psi}\psi]$ has the correct scaling behavior in $(T - T_c)/T_c$.

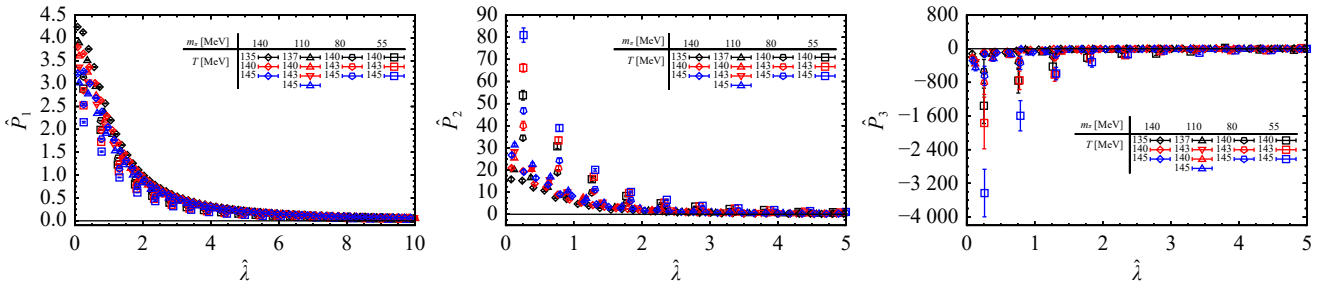


Fig. 5 \hat{P}_n as function of $\hat{\lambda} \equiv \lambda/m$ for $n=1$ (left), $n=2$ (middle) and $n=3$ (right) with pion mass ranging from 140 to 55 MeV in the proximity of T_c . The plots are taken from Ref. [10]. (color online)

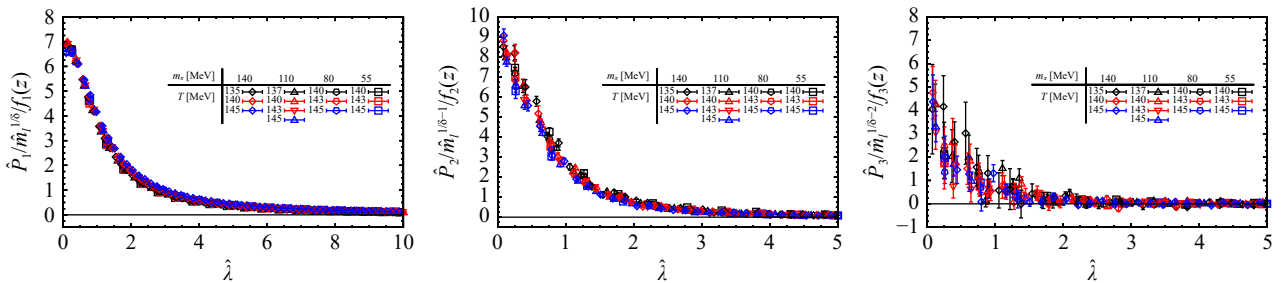


Fig. 6 Similar as Fig. 5 but for $\hat{P}_n/\hat{m}_l^{1/\delta-n+1}/f_n(z)$. The plots are taken from Ref. [10]. (color online)

3 Summary

In this contribution we review our recent work on the microscopic origin of the axial U(1) anomaly at $1.6 T_c$ as

well as the macroscopic criticality of chiral phase transition in the proximity of T_c ^[9–10]. To access the quark mass dependence of the Dirac eigenvalue spectrum $\rho(\lambda)$ a novel method to compute the quark mass derivative of $\rho(\lambda)$

was proposed [Eqs. (6)~(7)]. By investigating on the first, second and third order derivatives of $\rho(\lambda)$ with respect to quark mass from lattice QCD simulations with pion mass down to 55 MeV on $N_\tau = 8, 12$ and 16 lattices it is found that it is $\rho(\lambda) \propto m^2 \delta(\lambda)$ that breaks the axial U(1) symmetry and restores the $SU(2) \times SU(2)$ chiral symmetry at $1.6 T_c$. This is consistent with the dilute instanton gas approximation and also the observation of $\chi_\pi - \chi_\delta = \chi_{\text{disc}} \neq 0$ in the chiral and continuum limit at $1.6 T_c$. These findings suggests the axial U(1) anomaly still remains manifested at T_c , which is lower than $1.6 T_c$. Thus the chiral phase transition should be of second order belonging to the O(4) universality class.

The relation between n th order cumulant of chiral condensate $\mathbb{K}_n[\bar{\psi}\psi]$ and the correlation between Dirac eigenvalue spectrum $P_n(\lambda)$ has been established [Eq. (17)]. Accordingly the Banks-Casher relation is generalized [Eq. (21)]. Based on these relations it is conjectured that $\mathbb{K}_n[\bar{\psi}\psi] \propto h^{1/\delta-n+1} f_n(z)$ and $P_n(\lambda) = h^{1/\delta-n+1} f_n(z)g(\lambda/m)$. By performing lattice QCD simulations using HISQ fermions with pion mass ranging from 140 MeV to 55 MeV on $N_\tau = 8$ lattices in the proximity of chiral phase transition the conjecture is confirmed for n up to 3.

Since the manifestation of the axial U(1) anomaly at a high temperature of $1.6 T_c$ and the chiral phase transition near T_c have been demonstrated microscopically, it would be interesting to investigate the temperature range between $1.6 T_c$ and T_c in the near future. Specifically, examining how the dilute instanton gas approximation breaks down and transitions to the scenario of the chiral phase transition could provide valuable insights into the nature of the QCD transition. Additionally, exploring the connection between the Dirac eigenvalue spectrum and other thermodynamic quantities would be highly worthwhile.

Acknowledgments I thank Wei-Ping Huang for his assistance in producing Fig. 1 and Table 1. This material is based upon work supported partly by the National Key Research and Development Program of China under Contract No. 2022YFA1604900; the National Natural Science Foundation of China under the grant numbers 12293064, 12293060 and 12325508.

References:

- [1] PISARSKI R D, WILCZEK F. *Phys Rev D*, 1984, 29: 338.
- [2] DING H T, KARSCH F, MUKHERJEE S. *Int J Mod Phys E*, 2015, 24(10): 1530007.
- [3] DING H T. *Nucl Phys A*, 2021, 1005: 121940.
- [4] AOKI Y, ENDRODI G, FODOR Z, et al. *Nature*, 2006, 443: 675.
- [5] BAZAVOV A, DING H T, HEGDE P, et al. *Phys Lett*, 2019, B795: 15.
- [6] BORSANYI S, FODOR Z, GUENTHER J N, et al. *Phys Rev Lett*, 2020, 125(5): 052001.
- [7] DING H T, HEGDE P, KACZMAREK O, et al. *Phys Rev Lett*, 2019, 123(6): 062002.
- [8] AARTS G, AICHELIN J, ALLTON C, et al. *Prog Part Nucl Phys*, 2023, 133: 104070.
- [9] DING H T, LI S T, MUKHERJEE S, et al. *Phys Rev Lett*, 2021, 126(8): 082001.
- [10] DING H T, HUANG W P, MUKHERJEE S, et al. *Phys Rev Lett*, 2023, 131(16): 161903.
- [11] BUTTI A, PELISSETTO A, VICARI E. *JHEP*, 2003, 08: 029.
- [12] PELISSETTO A, VICARI E. *Phys Rev D*, 2013, 88(10): 105018.
- [13] GRAHL M. *Phys Rev D*, 2014, 90(11): 117904.
- [14] OHNO H, HELLER U M, KARSCH F, et al. *PoS*, 2012, LATTICE2012: 095.
- [15] COSSU G, AOKI S, FUKAYA H, et al. *Phys Rev D*, 2013, 87(11): 114514.
- [16] CHIU T W, CHEN W P, CHEN Y C, et al. *PoS*, 2014, LATTICE2013: 165.
- [17] DICK V, KARSCH F, LAERMANN E, et al. *Phys Rev D*, 2015, 91(9): 094504.
- [18] TOMIYA A, COSSU G, AOKI S, et al. *Phys Rev D*, 2017, 96(3): 034509.
- [19] BRANDT B B, FRANCIS A, MEYER H B, et al. *JHEP*, 2016, 12: 158.
- [20] SUZUKI K, AOKI S, AOKI Y, et al. *PoS*, 2020, LATTICE2019: 178.
- [21] LAHIRI A. *PoS*, 2022, LATTICE2021: 003.
- [22] DING H T, LI S T, WANG X D, et al. *PoS*, 2022, LATTICE2021: 619.
- [23] DING H T, HUANG W P. *Scientia Sinica Physica, Mechanica & Astronomica*, 2023, 53(9): 290004.
- [24] DING H T, KACZMAREK O, KARSCH F, et al. *PoS*, 2020, LATTICE2019: 251.
- [25] GIUSTI L, LUSCHER M. *JHEP*, 2009, 03: 013.
- [26] COSSU G, FUKAYA H, HASHIMOTO S, et al. *PTEP*, 2016, 2016(9): 093B.
- [27] FODOR Z, HOLLAND K, KUTI J, et al. *PoS*, 2016, LATTICE2015: 310.
- [28] DING H T, LI S T, TOMIYA A, et al. *Phys Rev D*, 2021, 104(1): 014505.
- [29] KACZMAREK O, KARSCH F, LAERMANN E, et al. *Phys Rev D*, 2011, 83: 014504.
- [30] DING H T, KACZMAREK O, KARSCH F, et al. *Phys Rev D*, 2024, 109(11): 114516.
- [31] EJIRI S, KARSCH F, LAERMANN E, et al. *Phys Rev D*, 2009, 80: 094505.
- [32] CLARKE D A, KACZMAREK O, KARSCH F, et al. *Phys Rev D*, 2021, 103(1): L011501.

量子色动力学手征相变及其微观起源

丁亨通¹⁾

(华中师范大学夸克与轻子物理教育部重点实验室和粒子物理研究所, 武汉 430079)

摘要: 强相互作用主导的核物质从强子相到夸克-胶子等离子体相的转变是一个快速的平滑过渡, 而不是真实意义上(即存在发散临界行为)的相变。量子色动力学真实意义上的相变只存在于某些特定的极限中, 比如夸克质量为零的手征极限等极限条件。在本工作中将展示我们最近关于手征相变及其微观起源的研究。这些研究均基于(2+1)-味的、采用了高度改进的交错费米子的、 π 介子质量为 160 MeV 到 55 MeV 的格点量子色动力学模拟。基于新提出的方法计算格点上 Dirac 本征值谱的夸克质量导数, 发现轴 U(1) 反常在 $1.6 T_c$ 时仍然存在, 其微观起源与稀疏瞬子气体近似相一致。此外, 基于格点 QCD 结果和提出的广义 Banks-Casher 关系, 发现手征相变的宏观奇异性体现在 Dirac 本征值谱的关联之中。对未来相关研究方向做了展望, 包括研究温度在 T_c 到 $1.6 T_c$ 之间的 QCD 相变行为来理解稀疏瞬子气体近似的失效及其与手征相变的联系。

关键词: 量子色动力学相结构; 狄拉克本征值谱; 手征反常; 手征对称性; 临界行为

收稿日期: 2023-10-02; 修改日期: 2024-02-27

基金项目: 国家重点研发计划项目(2022YFA1604900); 国家自然科学基金资助项目(12293064, 12293060, 12325508)

1) E-mail: hengtong.ding@ccnu.edu.cn